Research Article

Journal of Physical Organic Chemistry

Received: 7 December 2007, Revised: 25 January 2008, Accepted: 25 January 2008, Published online in Wiley InterScience: 2008

(www.interscience.wiley.com) DOI 10.1002/poc.1350

Theoretical study of racemization in chiral alkenylidene truxenes

Ibon Alkorta[a]*, Fernando Blanco[a] and José Elguero[a]

DFT based methods have been used to study the racemization process of chiral truxene derivatives. Four minima and the transition state connecting them have been characterized. It has been found that the energetic results for the transition states are correlated for each compound and also among the different systems considered. Thus, a unique equation has been found to fit all the values obtained. Model systems have shown that the calculated barriers are not inherent to the truxene structure. The AIM analysis has shown the presence of a large number of intramolecular closed-shell interactions while electron density and Laplacian at the bond critical points are exponentially correlated with the interatomic distance. Copyright © 2008 John Wiley & Sons, Ltd.

Keywords: truxenes; DFT; optical rotatory power

INTRODUCTION

Truxene derivatives present an overlap of the supramolecular and fullerene chemistry fields. Thus, the concave shape of truxene derivatives make them suitable intermediates for the total synthesis of fullerenes[1–3] and, adequately functionalized, as supramolecular partners in the recognition of fullerene derivatives.[4] The chiral properties of some truxenes result from their concave shape that provides axial chirality to the molecules. This property offers great opportunities in the selective molecular recognition of chiral guests with axial chirality.

In general, the synthetic methods used to obtain truxenes provide racemic mixtures of these compounds. Thus, very little information is available on the chiral properties of these systems.

To the best of our knowledge, no theoretical or experimental work has been carried out on the potential energy surface of these systems. Thus, a theoretical analysis of them and the barriers of their chiral racemization appear to be of interest. In the present paper, the minima and transition states of a series of chiral alkenylidene truxenes have been characterized and their geometrical and electronic properties analyzed. In addition, the evolution of the optical rotatory power along the reaction coordinate has been evaluated.

METHODS

The geometry of the systems has been fully optimized with the DFT based method, B3LYP[5,6] and the 6-31G(d) basis set[7] within the Gaussian-03 package.[8] Frequency calculations have been carried out at the same computational level to confirm that the structures obtained correspond to minima (**min**) or to transition states (**ts**). The optical rotatory power has been calculated using the GIAO orbitals. The calculated optical rotation corresponds to the sodium D line frequency, $[\alpha]_D$. The effect of the solvation in the relative energy of the structures has been evaluated using the PCM solvent model to simulate water as solvent.[9] The electron density properties of the systems have been analyzed within the Atoms In Molecules theory (AIM)[10,11] with the PROAIMV,[12] MORPHY98[13] and AIM2000 programs.[14]

RESULTS AND DISCUSSION

Energy and geometry

The molecules considered are represented in Scheme 1. In the case of the truxenone, X = O, a unique minimum has been found having planar C_{3h} symmetry. In the rest of the cases, four minima were found (Scheme 2), which base on the disposition of the external aromatic rings A-C above, *u*, or below, *d*, the plane of the central aromatic ring D, can be defined as *uuu, uud, udd* and *ddd*, being, *uuu/ddd* (**min1**/**min4**) and *uud/udd* (**min2**/**min3**) two pairs of enantiomers. **Min1** presents a C_3 symmetry in all the cases considered with the external aromatic ring above the plane of the central ring and the X groups below the same reference plane (Fig. 1). **Min2** shows C_1 symmetry.

Three transition states, **ts1–ts3**, connect the stepwise transformation of the minima structure from **min1** to **min4**, presenting in each case a planar or quasi-planar configuration of the external aromatic rings, *p*. Again, **ts1/ts3** are enantiomeric structures. These three **ts** present C_1 symmetry. The possibility of a simultaneous conversion of the three external aromatic rings from **min1** to **min4**, from *uuu* to *ddd*, has been considered, **ts4**. This planar structure has C_{3h} symmetry for all the molecules considered here and presents up to six imaginary frequencies and thus, it is not a true **ts**.

* *Instituto de Química Médica (C.S.I.C.), Juan de la Cierva, 3, E-28006-Madrid, Spain.*
E-mail: ibon@iqm.csic.es

a *I. Alkorta, F. Blanco, and J. Elguero*
Instituto de Química Médica (C.S.I.C.), Juan de la Cierva, 3, E-28006-Madrid, Spain

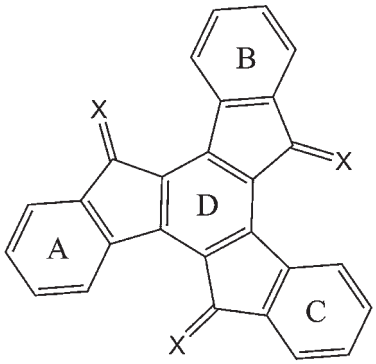

1, X = O, S, CH_2, CHF, CF_2, CCl_2

Scheme 1. Truxenes studied

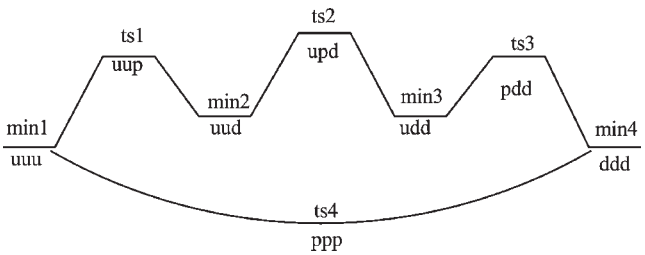

Scheme 2. Minima and **ts** characterized in the energy potential surface

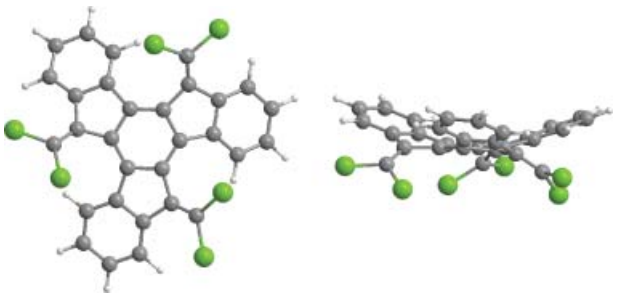

Figure 1. Two views of the **min1** of the hexachloro derivative, X = CCl_2.

In all cases, the most stable minimum corresponds to **min1** (or **min4**) (Table 1 and Fig. 2). The relative energy of **min2** increases with the size of the substituents, thus, the differences goes from 6.1 to 10.7 and 27.1 for the derivatives with CH_2, CF_2 and CCl_2 substituents. The presence of F atom in *E* or *Z* configuration in the CHF derivatives clearly indicates that the main responsible of the energetic barrier is the one in the ZZZ configuration since its values are similar to the CF_2 derivatives. In contrast, the results obtained for the CHF(*EEE*) are analogous to the CH_2 one.

The barriers found in **ts1** and **ts2** for a given compound are similar being, in all the cases studied, **ts2** smaller than **ts1**. As expected, the effect of the substituents is even more dramatic here than in the minima. Thus, the barrier of **ts1** increases from 18.2 to 42.6 and 114.6 when the X groups are CH_2, CF_2 and CCl_2, respectively.

The barrier found for **ts4** is always much higher than those corresponding to **ts1** and **ts2**. These results indicate that the transformation of **min1** in **min4** will proceed stepwise instead of in a single step. The three **ts** barriers calculated are highly correlated as shown in Eqn 1 and 2, where **ts1** has been used to compare the other two. These results indicate that a similar mechanism operate in all the cases, modulated by the different characteristics of the substituents.

Table 1. Total energy (hartree) of the **min1** configuration and relative energy of the rest of the structures (kJ mol^{-1}) of **1**

X	min1	ts1	min2	ts2	ts4
O	−1261.81890				
S	−2230.67299	2.97	1.85	2.24	14.17
CH_2	−1154.01734	18.18	6.10	17.13	75.63
CHF(*EEE*)	−1451.71276	21.11	5.70	18.93	95.78
CHF(ZZZ)	−1451.70296	31.47	10.57	27.05	142.69
CF_2	−1749.41837	42.65	10.70	34.03	231.45
CCl_2	−3911.53970	114.56	27.08	88.25	615.89

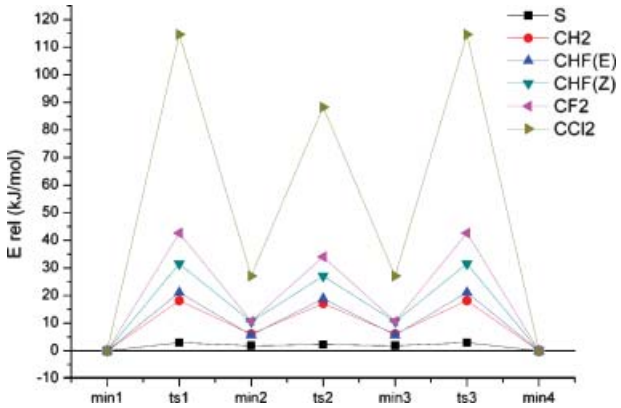

Figure 2. Energetic profile of the stationary points considered

$$0.79 * E(\mathbf{ts1}) = E(\mathbf{ts2}),\ n = 6,\ R^2 = 0.995 \quad (1)$$

$$5.28 * E(\mathbf{ts1}) = E(\mathbf{ts4}), n = 6, R^2 = 0.994 \quad (2)$$

From Eqn. 1 and 2, the value of **ts1** can be arbitrarily fixed to 1 and thus **ts2** and **ts4** become 0.79 and 5.28. Using these values, the group contributions are calculated as: S 2.70; CH_2 14.61; CHF-*E* 18.36; CHF-*Z* 27.33; CF_2 43.78, and CCl_2 116.47 kJ mol^{-1}.

The product of the value of a given **ts** and the corresponding group provide an estimate of the **ts** barrier (the calculated and estimated values present an R^2 of 0.9996).

In order to evaluate if the **ts** barriers are or not intrinsic to the structure of the truxene derivatives, the molecules shown in Scheme 3 have been examined. Molecule **2** with X = O and S present a C_s minimum geometry while in the rest of the cases the minimum is non-planar and thus, they are chiral. The racemization barriers obtained for **2** are of the same order of magnitude as those obtained for **1** but always slightly smaller, being the barriers found for **2** linearly correlated with those of **1**. Thus, these model compounds are able to explain the barrier observed in **1** (Table 2)

Journal of Physical Organic Chemistry

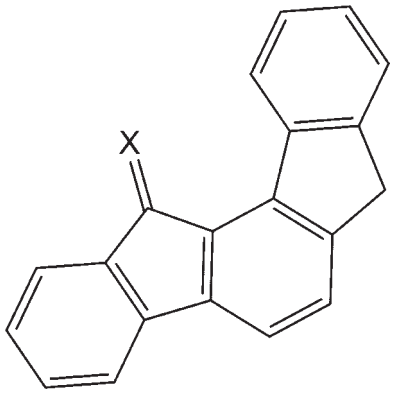

2

$X = O, S, CH_2, CF_2, CCl_2$

Scheme 3. Simplified model of truxene

Table 2. Total energy (hartree) of the **minima**, **ts** barrier (kJ mol^{-1}) and symmetry of the **ts** structure of **2**

X	**Minimum**	**ts**	Symmetry of **ts**
O	−844.61303	0.0*	—
S	−1167.56699	0.0*	—
CH_2	−808.679518	7.94	C_s
CF_2	−1007.14635	23.47	C_s
CCl_2	−1727.85208	85.80	C_1

* Minimum is a planar structure.

Table 3. Geometrical parameters*

	Angles between the aromatic ring D with			Distance between the aromatic centre and the plane of D		
X	A	B	C	A	B	C
S (**min1**)	12.1	12.1	12.1	0.286	0.286	0.286
S (**ts1**)	18.6	7.7	−5.5	0.453	0.349	0.281
S (**min2**)	18.9	9.4	−12.0	0.506	0.276	−0.593
S (**ts2**)	16.5	−14.9	−10.3	0.663	−0.153	−0.489
CH_2 (**min1**)	13.3	13.3	13.3	0.383	0.383	0.383
CH_2 (**ts1**)	18.4	8.9	−1.8	0.517	0.376	−0.089
CH_2 (**min2**)	20.1	5.8	−10.4	0.571	0.282	−0.504
CH_2 (**ts2**)	18.4	−14.0	−8.4	0.747	−0.127	−0.448
CHF(*E*) (**min1**)	13.3	13.3	13.3	0.369	0.369	0.369
CHF(*E*) (**ts1**)	18.4	9.3	−2.2	0.497	0.378	−0.088
CHF(*E*) (**min2**)	20.1	6.1	−10.8	0.551	0.299	−0.510
CHF(*E*) (**ts2**)	18.9	−14.9	−9.0	0.767	−0.093	−0.469
CHF(*Z*) (**min1**)	15.9	15.9	15.9	0.553	0.553	0.553
CHF(Z) (**ts1**)	21.3	10.5	−0.7	0.708	0.465	−0.054
CHF(Z) (**min2**)	23.7	5.5	−10.6	0.825	0.232	−0.531
CHF(Z) (**ts2**)	22.3	−18.7	−8.0	0.992	−0.351	−0.426
CF_2 (**min1**)	16.0	16.0	16.0	0.556	0.556	0.556
CF_2 (**ts1**)	21.4	12.3	−1.9	0.694	0.537	−0.025
CF_2 (**min2**)	23.6	5.6	−11.1	0.810	0.256	0.534
CF_2 (**ts2**)	24.0	−8.7	−20.9	1.075	−0.451	−0.330
CCl_2 (**min1**)	22.7	22.7	22.7	0.886	0.886	0.886
CCl_2 (**ts1**)	26.7	19.0	9.6	1.015	0.633	0.295
CCl_2 (**min2**)	31.6	2.4	−8.9	1.234	0.027	−0.456
CCl_2 (**ts2**)	39.3	−6.4	−35.5	1.698	−0.307	−0.824

* Negative values in the distance indicate that the corresponding aromatic ring is below the plane of ring D.

Among the calculated compounds, the experimental X-ray geometry is only available for $X = CCl_2$ (ref. code TIWVAW[15] of the CSD database[16]). It presents a configuration analogous to that of **min1**, being the dihedral angle of the average plane of the external aromatic rings with the central one 21.4° (22.7° in the calculated structure).

In Table 3, the dihedral angle of the plane of the aromatic rings A-C with the plane of D and the distance of the centre of the rings A-C to the plane of D have been gathered. The dihedral angle provides information of the inclination of the A-C rings with respect of D, while the distance of the centre of A-C rings to the plane of D provides an idea of the curvature of the truxene derivative. Thus, as the size of the substituents increases, the value of the distance in **min1** increases. As in the case of the energies, the CHF(*E*) derivative presents values similar to the CH_2 and the CHF(*Z*) to the CF_2 one.

Another interesting effect of the **ts** is the distortion of the bond angle in the X substituents than can reach as much as 15° in the **ts4** with respect to those obtained in the minima. This effect is a consequence of the molecule trying to reduce the direct interaction of the atoms of X with the hydrogen atoms of the adjacent aromatic ring.

The volume of the different configurations reported in this paper has been calculated as defined by an isoelectronic surface with a value of 0.001 a.u. The results (Table 4) show that **min1** is the smaller configuration in two cases, $X = CH_2$ and CF_2, while **min2** is the smaller for X = S and CHF(*EEE*), in the case of CHF(ZZZ) and CCl_2 the minimum volume configuration corresponds to a **ts** structure. It is significant that the structure of **ts4**,

Table 4. Total volume of **min1** and relative for the rest of the configurations (a.u.)

X	**min1**	**ts1**	**min2**	**ts2**	**ts4**
S	3213.3	16.8	−38.4	58.1	23.5
CH_2	3109.0	25.6	129.0	66.1	91.0
CHF(*EEE*)	3148.3	42.1	−19.9	10.0	143.1
CHF(*ZZZ*)	3134.0	43.9	136.8	−53.7	142.2
CF_2	3163.5	80.4	55.3	81.4	190.7
CCl_2	3827.3	−263.2	116.8	−63.3	17.5

	min	**ts**
2 ($X = CH_2$)	2313.5	−66.0
2 ($X = CF_2$)	2355.6	−51.6
2 ($X = CCl_2$)	2442.1	73.6

Table 5. Solvation free energy (kJ mol^{-1}) of **min1** and relative energy (kJ mol^{-1}) of the rest of the structures including the solvation

		Solvation	Erel*			
X	Solvent	**min1**	**ts1**	**min2**	**ts2**	**ts4**
S	H_2O	15.61	4.59	3.69	4.30	19.05
CH_2	C_6H_6	27.48	17.25	5.25	16.39	73.08
CH_2	CH_3COCH_3	3.90	16.88	6.67	15.79	70.96
CH_2	H_2O	36.57	16.70	5.54	15.77	69.75
CHF(*E*)	H_2O	31.18	19.96	5.39	17.79	91.88
CHF(*Z*)	H_2O	17.59	32.56	10.42	28.30	146.54
CF_2	H_2O	37.82	42.44	10.00	34.39	228.93
CCl_2	H_2O	45.09	114.75	27.39	88.57	604.38

* The energy value of **min1** has been used as reference for the rest of the configurations of each molecule.

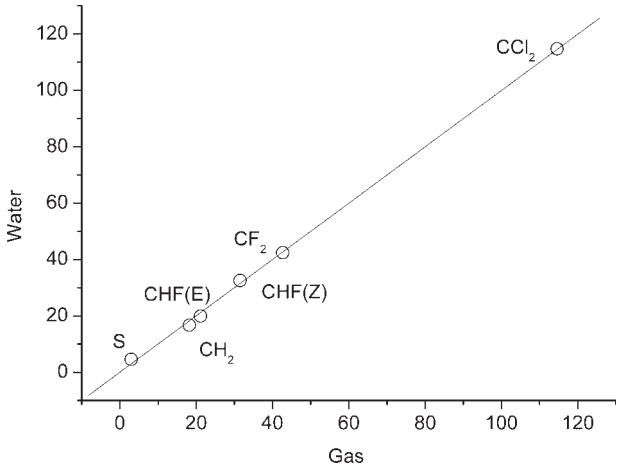

Figure 3. Effect of water solvent on **ts1**

which corresponds to a C_{3h} symmetry configuration, is never the smallest and in several cases it is the largest of the considered conformations. However, it should be noted that this volume corresponds to the isolated molecules in gas phase and it is very different from the apparent size in condensed phase that depends on the ability of the molecules to complement each other.

Solvation

The effect of the relative stability of the **minima** and the **ts** barrier has been evaluated using the PCM continuum solvent model. For one of the cases (X = CH_2), three solvents have been considered, benzene, acetone and water. The chosen solvents have been selected based on their different complexation characteristics and range of dielectric constants (2.247, 20.7 and 78.39, respectively) (Table 5). The results show that the solvation is very similar for all the structures of this compound in a given solvent. For the rest of the compounds, only the more polar solvent has been considered. Again, the energetic profile obtained in vacuum is similar to the one obtained with the solvation model.

The calculated values of the solvation free energy show very unfavourable values, that is, large increases in the values for the water solvent model in all the cases studied. In the case of the hydrocarbon, X = CH_2, both the solvation in water and benzene are very unfavourable while acetone as solvent seems to be only slightly unfavourable.

If one compares **ts1** without (Table 1) and with water solvation (Table 5) the plot represented in Fig. 3 is obtained. It shows that gas phase calculation in truxenes can be used to compare with future experimental barriers.

Analysis of the electron density (AIM)

The analysis of the electron density within the AIM methodology shows the presence of bond critical points (bcp) between the X substituents and the surrounding aromatic moieties of these molecules (Fig. 4). Thus, H···H, H···F, Cl···H and S···H interactions are obtained which present small values of the electron density at

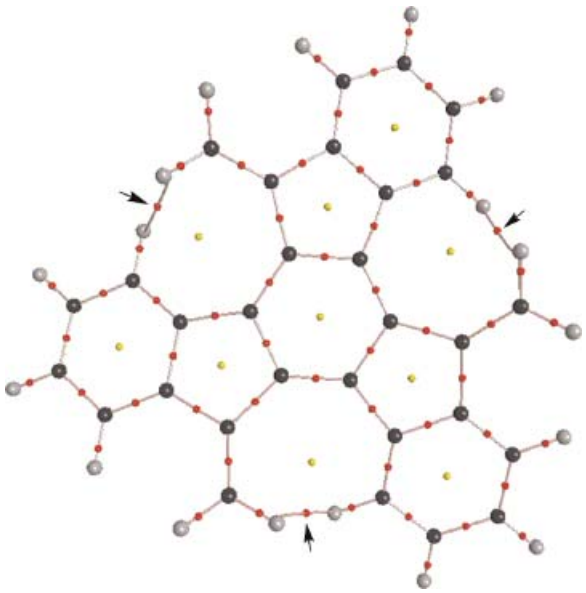

Figure 4. Molecular graph of **min1** of X = CH_2. The bond critical points are shown in red and the ring critical points in yellow. The closed shell interactions are indicated with arrows.

the bond critical point and positive values of the Laplacian. In some isolated cases other interactions are found with the carbon atoms of the aromatic rings. The values of the electron density and its Laplacian at the bond critical points correlate exponentially with the interatomic distance of the atoms involved (Fig. 5 and Eqns 3–10). Similar results have been already described for other closed shell interactions.[17–19]

$$0.3527 * \exp(-0.873 * \text{distance}) = (\text{H}\cdots\text{H contacts})\ \rho_{bcp},\ R^2 = 0.9866,\ n = 41 \quad (3)$$

$$0.3288 * \exp(-0.4794 * \text{distance}) = \nabla^2\rho_{bcp},\ R^2 = 0.9188 \quad (4)$$

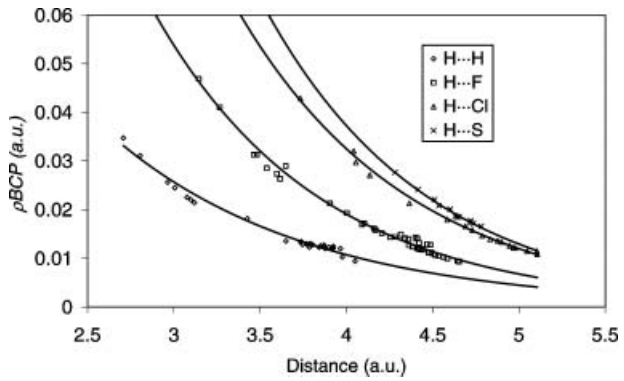

Figure 5. Electron density at the bond critical point, ρ_{bcp}, *versus* the interatomic distance. The fitted curves are those of Eqns 3, 5, 7 and 9

$$1.2054 * \exp(-1.0363 * \text{distance}) = (\text{H}\cdots\text{F contacts})\ \rho_{bcp},\ R^2 = 0.9889,\ n = 59 \quad (5)$$

$$3.0774 * \exp(-0.9077 * \text{distance}) = \nabla^2 \rho_{bcp},\ R^2 = 0.9691 \quad (6)$$

$$1.7644 * \exp(-0.9985 * \text{distance}) = (\text{H}\cdots\text{Cl contacts})\ \rho_{bcp},\ R^2 = 0.9973,\ n = 24 \quad (7)$$

$$3.3656 \exp(-0.8483 * \text{distance}) = \nabla^2 \rho_{bcp},\ R^2 = 0.9807 \quad (8)$$

$$2.5723 * \exp(-1.0587 * \text{distance}) = (\text{H}\cdots\text{S contacts})\rho_{bcp},\ R^2 = 0.9951,\ n = 16 \quad (9)$$

$$1.2151 \exp(-0.6573 * \text{distance}) = \nabla^2 \rho_{bcp},\ R^2 = 0.9727 \quad (10)$$

For the same distance, the values of the H···S contacts are larger than those of the H···Cl ones.

Optical rotatory power

The calculated optical rotatory power (ORP) presents very large values for the **min1** that decreases steadily in **ts1**, **min2** and are very small in **ts2** (Table 6). It should be noted that **ts2** represents the geometry where these system energetically change from one enantiomer to its opposite but instead of using a symmetric path used a non-symmetric one and thus, this structure present a small ORP value. The values obtained provide a measure of the chirality of the structures for a given derivative.

In addition, the similar behaviour of this property in all the compounds studied is confirmed by a high correlation coefficient between the data shown in Table 6 (the smallest R^2 value obtained in all the possible correlations is 0.94)

Table 6. Optical rotatory power, $[\alpha]_D$, (°) of the chiral configurations of **1**

	min1	ts1	min2	ts2
S	2111.33	1268.61	345.46	−69.37
CH_2	1808.68	1252.81	532.21	43.52
CHF(*E*)	1613.13	1158.92	468.78	37.12
CHF(*Z*)	1464.87	967.66	438.49	126.85
CF_2	1330.21	905.76	403.25	104.08
CCl_2	1705.25	1410.68	534.25	24.8

CONCLUSIONS

A theoretical study of the potential energy surface of a series of chiral truxene derivatives has been carried out by means of DFT calculation methods. Four minima and four transition states have been characterized. A step-wise transformation between the two enantiomeric structures with C_3 symmetry is able to explain the configurations found. The synchronous transition state barrier presents much larger energy than the step-wise and thus is not feasible for most of the system considered.

In all the cases, the most stable **minima** correspond to that with a C_3 symmetry and the **ts** barriers are related to the size of the substituents, especially to those located *Z* to the double bond. The calculated solvation energy does not affect significantly the relative energies of the configurations obtained.

The analysis of the electron density shows the presence of closed shell intramolecular interactions. Exponential relationships have been found between the value of the electron density and its Laplacian *versus* the interatomic distance of the atoms involved.

The calculated ORP of the different configurations provides a qualitative idea of the chirality of the structures, thus, the larger values are obtained for **min1** and then decrease up to **ts2** where the values are close to zero.

SUPPORTING INFORMATION

Geometry of all the stationary points (minima and TS) calculated at the B3LYP/6-31G* computational level.

Acknowledgements

This work was carried out with financial support from the Ministerio de Educación y Ciencia (Project No. CTQ2006-14487-C02-01/BQU) and Comunidad Autónoma de Madrid (Project MADRISOLAR, ref. S-0505/PPQ/0225). Thanks are given to the CTI (CSIC) and CESGA for allocation of computer time.

REFERENCES

[1] B. Gómez-Lor, O. de Frutos, A. M. Echavarren, *Chem. Commun.* **1999**, 2431–2432.
[2] B. Gómez-Lor, C. Koper, R. H. Fokkens, E. J. Vlietstra, T. J. Cleij, L. W. Jenneskens, N. M. M. Nibbering, A. M. Echavarren, *Chem. Commun.* **2002**, 370–371.
[3] B. Gómez-Lor, E. González-Cantalapiedra, M. Ruiz, S. de Frutos, D. J. Cárdenas, A. Santos, A. M. Echavarren, *Chem. Eur. J.* **2004**, *10*, 2601–2608.
[4] E. M. Pérez, M. Sierra, L. Sánchez, M. R. Torres, R. Viruela, P. M. Viruela, E. Ortí, N. Martín, *Angew. Chem. Int. Edit.* **2007**, *46*, 1847–1851.
[5] A. D. Becke, *J. Chem. Phys.* **1993**, *98*, 5648–5652.
[6] C. T. Lee, W. T. Yang, R. G. Parr, *Phys. Rev. B* **1988**, *37*, 785–789.

[7] P. C. Hariharan, J. A. Pople, *Theor. Chim. Acta* **1973**, *28*, 213–222.
[8] M. J. Frisch, G. W. Trucks, H. B. Schlegel, G. E. Scuseria, M. A. Robb, J. R. Cheeseman, T. Montgomery, J. A, T. Vreven, K. N. Kudin, J. C. Burant, J. M. Millam, S. S. Iyengar, J. Tomasi, V. Barone, B. Mennucci, M. Cossi, G. Scalmani, N. Rega, G. A. Petersson, H. Nakatsuji, M. Hada, M. Ehara, K. Toyota, R. Fukuda, J. Hasegawa, M. Ishida, T. Nakajima, Y. Honda, O. Kitao, H. Nakai, M. Klene, X. Li, J. E. Knox, H. P. Hratchian, J. B. Cross, V. Bakken, C. Adamo, J. Jaramillo, R. Gomperts, R. E. Stratmann, O. Yazyev, A. J. Austin, R. Cammi, C. Pomelli, J. W. Ochterski, P. Y. Ayala, K. Morokuma, G. A. Voth, P. Salvador, J. J. Dannenberg, V. G. Zakrzewski, S. Dapprich, A. D. Daniels, M. C. Strain, O. Farkas, D. K. Malick, A. D. Rabuck, K. Raghavachari, J. B. Foresman, J. V. Ortiz, Q. Cui, A. G. Baboul, S. Clifford, J. Cioslowski, B. B. Stefanov, G. Liu, A. Liashenko, P. Piskorz, I. Komaromi, R. L. Martin, D. J. Fox, T. Keith, M. A. Al-Laham, C. Y. Peng, A. Nanayakkara, M. Challacombe, P. M. W. Gill, B. Johnson, W. Chen, M. W. Wong, C. Gonzalez, J. A. Pople, Gaussian-03. Gaussian, Inc., Wallingford CT, **2003**.
[9] S. Miertus, E. Scrocco, J. Tomasi, *Chem. Phys.* **1981**, *55*, 117–129.
[10] R. F. W Bader, *Atoms in Molecules: A Quantum Theory* (The International Series of Monographs of Chemistry). Clarendon Press, Oxford, **1990**.
[11] P. L. A. Popelier, *Atoms in Molecules: an Introduction*, Prentice Hall, Harlow, England, **2000**.
[12] F. W. Biegler-König, R. F. W. Bader, T. H. Tang, *J. Comput. Chem.* **1982**, *3*, 317–328.
[13] P. L. A. Popelier, With a contribution from R.G.A. Bone (UMIST, Engl, EU) MORPHY98, a topological analysis program, **1999**.
[14] F. W. Biegler-König, J. Schönbom, AIM2000, Bielefeld, Germany, **2002**.
[15] F. Sbrogio, F. Fabris, O. Delucchi, G. Valle, *Gazz. Chim. Ital.* **1995**, *125*, 623–625.
[16] F. H. Allen, J. E. Davies, J. J. Galloy, O. Johnson, O. Kennard, C. F. Macrae, E. M. Mitchell, G. F. Mitchell, J. M. Smith, D. G. Watson, *J. Chem. Inf. Comp. Sci.* **1991**, *31*, 187–204.
[17] I. Alkorta, I. Rozas, J. Elguero, *Struct. Chem.* **1998**, *9*, 243–247.
[18] I. Alkorta, L. Barrios, I. Rozas, J. Elguero, *J. Mol. Struc.: Theochem.* **2000**, *496*, 131–137.
[19] E. Espinosa, I. Alkorta, J. Elguero, E. Molins, *J. Chem. Phys.* **2002**, *117*, 5529–5542.